Acta Astronautica 68 (2011) 1761–1773

Contents lists available at ScienceDirect

Acta Astronautica

journal homepage: www.elsevier.com/locate/actaastro

Two-craft tether formation relative equilibria about circular orbits and libration points

Ravi Inampudi *, Hanspeter Schaub [1]

Aerospace Engineering Sciences Department, University of Colorado, Boulder, CO, United States

ARTICLE INFO

Article history:
Received 7 September 2010
Received in revised form
2 February 2011
Accepted 2 February 2011
Available online 26 February 2011

Keywords:
Satellite formation flying
Great-circle and nongreat-circle relative equilibria
Circular Earth orbit
Libration points

ABSTRACT

The relative equilibria of a two spacecraft tether formation connected by line-of-sight elastic forces moving in the context of a restricted two-body system and a circularly restricted three-body system are investigated. For a two spacecraft formation moving in a central gravitational field, a common assumption is that the center of the circular orbit is located at the primary mass and the center of mass of the formation orbits around the primary in a great-circle orbit. The relative equilibrium is called great-circle if the center of mass of the formation moves on the plane with the center of the gravitational field residing on it; otherwise, it is called a nongreat-circle orbit. Previous research shows that nongreat-circle equilibria in low Earth orbits exhibit a deflection of about a degree from the great-circle equilibria when spacecraft with unequal masses are separated by 350 km. This paper studies these equilibria (radial, along-track and orbit-normal in circular Earth orbit and Earth–Moon Libration points) for a range of inter-craft distances and semi-major axes of the formation center of mass. In the context of a two-spacecraft Coulomb formation with separation distances on the order of dozens of meters, this paper shows that the equilibria deflections are negligible (less than $10^{-6\circ}$) even for very heterogeneous mass distributions. Furthermore, the nongreat-circle equilibria conditions for a two spacecraft tether structure at the Lagrangian libration points are developed.

Published by Elsevier Ltd.

1. Introduction

This paper discusses the relative equilibria of two masses connected by a tether force moving in the presence of a central gravitational force field as well as the relative equilibria of such a formation at the libration points moving around the barycenter. The two masses are connected using a line-of-sight elastic force. For example, the two masses are either connected by a massless nonlinear spring or by a virtual electrostatic (Coulomb) force. Ref. [8] model the tether as a massless nonlinear spring and discusses the relative equilibria for long tethers on the order of hundreds of kilometers in a central gravitational field at low-earth orbits (LEO). This paper additionally investigates a Coulomb tether with inter-craft distances on the order of dozens of meters. In 2002, Ref. [1,2] introduced this novel method of exploiting Coulomb forces for formation flying control with separation distance on the order of dozens of meters. The Coulomb tether formation has several potential applications in space technologies, for example, high accuracy wide-field-of-view optical interferometry missions with geostationary orbits (GEO), spacecraft cluster control, as well as deployment or retrieval of dedicated sensors using Coulomb forces.

The relative equilibria of a two-craft formation at the libration points is also explored in this paper. In a circularly restricted three-body system, we consider a spacecraft formation near two large celestial objects

* Corresponding author.
E-mail addresses: inampudi@colorado.edu (R. Inampudi), hanspeter.schaub@colorado.edu (H. Schaub).
[1] H. Joseph Smead Fellow.

0094-5765/$ - see front matter Published by Elsevier Ltd.
doi:10.1016/j.actaastro.2011.02.003

which are rotating around their common center of mass. Due to the rotation of the system, there are five equilibrium points; these equilibrium points are the libration points (L_1–L_5) of the three-body system. Virtual Coulomb structures at the libration points are useful for remote-sensing missions to establish a long baseline imaging capability, or to ensure better stationkeeping configurations. Ref. [3] considers the equilibrium configurations of a rigid tethered system near all five libration points and carries out the stability analysis when it is near the translunar libration point. Ref. [4] presents the attitude dynamics and stability of a small rigid satellite in the vicinity of Lagrangian points. The paper also investigates the attitude dynamics of a satellite while it is in Lyapunov and halo orbits. Furthermore, the NIAC report in Ref. [1] analyzes the suitability of Coulomb control for a static collinear five-vehicle formation at Earth–Sun Lagrange points where the formation local dynamics ignore gravity.

In the context of a restricted two-body problem, the existence of great-circle relative equilibria for a satellite (spherically symmetric rigid body) implies that the center of the circular orbit coincides with the center of the gravitational field [5,6]. The dynamics of the satellite's center of mass is exactly that of the Keplerian point mass model. If the satellite is assumed to be an arbitrary rigid body, and making a first order approximation of the gravitational force acting on the rigid body assuming that the orbital motion is decoupled from the attitude motion, the classical rigid-body attitude equilibrium study reveals that all three rigid body principal axes must line up with the LVLH (local vertical/local horizontal) frame axes [7]. However, Ref. [5] uses the exact potential function expression and proves the existence of non-great-circle relative equilibria where the radius vector from the center of the gravitational field to the center of mass of the satellite traces a cone rather than a disk. Large variations in orientation from the classical regular motions are verified numerically for a finite rigid body [5].

Specifically, Ref. [8] discusses the relative equilibria and relative stability of a system of two spring-connected point masses moving in a central gravitational field. The paper shows that nongreat-circle equilibria exist for this simple spring system, and, for long tethers of approximately 3500 km at LEO, the attitude deflection from the vertical can reach tens of degrees. Such differences in orientation between great-circle and nongreat-circle solutions are particularly noticeable if the mass distribution of the formation is as asymmetric as possible. The spring system possesses $\boldsymbol{SO}(3)$ symmetry and such symmetry in geometric mechanics induces certain reduced dynamics which facilitates the computation of relative equilibria conditions. To obtain the conditions for relative equilibria, the principle of symmetric criticality is applied [8]. In order to gain further insights on the effects of nongreat-circle relative equilibria and mass asymmetry on a two spacecraft formation, the tether is modeled using a Coulomb force in this paper. The Coulomb formation has $\boldsymbol{SO}(3)$ symmetry as well.

There have been many interesting investigations on Coulomb formation dynamics [9–12]. Refs. [13–16] study static Coulomb structures where the differential gravitational forces between spacecraft are canceled through constant electrostatic forces. Thus, the open-loop equilibrium charges cause the virtual structure to assume a constant shape as seen by the rotating orbit frame. Some of these Coulomb concepts can have very asymmetric mass distributions. For example, consider the case of a small free-flying camera in the proximity of a large geostationary communication satellite. Because earlier work has shown that asymmetric bodies facilitate nongreat-circle equilibria, it is of interest how this impacts the 2-craft Coulomb virtual structure studies. The necessary conditions for a virtual Coulomb structure where the orbital motion is decoupled from the attitude motion are discussed in Ref. [13]. Refs. [14–16] search for static Coulomb structure solutions using genetic algorithms. Here the simple principle axes condition of rigid body equilibria are used to speed up the genetic search algorithms.

This paper investigates great-circle and nongreat-circle relative equilibria of a two spacecraft formation connected by any line-of-sight elastic force considering exact models for both the gravitational and tether potentials. Specifically, this paper presents the effects of nongreat-circle relative equilibria and mass asymmetry as a function of spacecraft separation distances (short to long tethers) and formation center of mass distances from low Earth orbits (LEO) to geostationary orbits (GEO). The aim is to identify for what formation dimension and altitudes these nongreat-circle effects become significant. This paper also investigates the validity of the principle axes condition assumption [13] for Coulomb tether applications taking nongreat-circle equilibria conditions into account. Moreover, this methodology is used to derive new two spacecraft formation relative equilibria conditions for a restricted three-body system at all five libration points.

In this paper, the following assumptions are made

1. The inter-spacecraft force undergoes both tensile and compressive forces along the line-of-sight direction between the two spacecraft.
2. The gravitational attraction between the two spacecraft masses is neglected.
3. For the three-body system, the spacecraft formation motion is in the plane of the motion of the primary bodies.

The paper is organized as follows. The system dynamics and the notion of $\boldsymbol{SO}(3)$ symmetry applied to an elastic tether formation moving in a central gravitational field as well as for a restricted three-body system are discussed. An example of modeling the tether force using Coulomb force is discussed. The principle of symmetric criticality is applied to determine the conditions of relative equilibria of such static structures. For the restricted two-body system, the reduced dynamics identifies the classical great-circle equilibria; radial, along-track and orbit normal equilibria. Also, the nongreat-circle effects in circular orbits for two-craft formations existing from LEO to GEO are investigated. Furthermore, relative equilibria solutions for a two spacecraft formation are derived at the libration points. Finally, the nongreat-circle equilibria effects of such formations are presented at L_1 and L_2 collinear libration points.

2. System description and *SO*(3) Symmetry

In the following sections, we introduce the fundamental concepts related to the dynamics of a system of N spacecrafts moving in a central gravitational field (restricted two-body system) and moving under the mutual gravitation of two bodies (restricted three-body system).

2.1. Restricted two-body system

The spacecrafts shown in the Fig. 1 are considered to be point masses moving in a central gravitational field. With the static virtual tether structure the system of spacecrafts behaves equivalently to a rigid body in orbit because the constant elastic inter-spacecraft forces cancel perfectly the differential gravitational forces acting across the cluster. Let $\boldsymbol{F}_t$ be the tether force acting between the two masses, and $\boldsymbol{r}_i$ be the inertial position vector of a single craft of mass m_i. Then the center of mass position vector $\boldsymbol{r}_c$ of this formation is defined as

$$\boldsymbol{r}_c = \frac{1}{M}\sum_{i=1}^{N} m_i \boldsymbol{r}_i \tag{1}$$

with $M = \sum_{i=1}^{N} m_i$ being the total formation mass. Let O be the center of the inverse square field and the origin of the inertial frame, while the formation's center of mass and center of gravity are denoted by C and G, respectively. The inertial position vectors of C and G are $\boldsymbol{r}_c$ and $\boldsymbol{r}_g$ and are related by

$$\boldsymbol{r}_g - \boldsymbol{r}_c = \boldsymbol{r} \tag{2}$$

where $\boldsymbol{r}$ is the constant vector between C and G.

From Newton's laws of gravitation the following relation relating the formation center of gravity and the individual inertial vectors is obtained as

$$\frac{\boldsymbol{r}_g}{\|\boldsymbol{r}_g\|^3} = \frac{1}{M}\sum_{i=1}^{N} \frac{\boldsymbol{r}_i}{\|\boldsymbol{r}_i\|^3} m_i \tag{3}$$

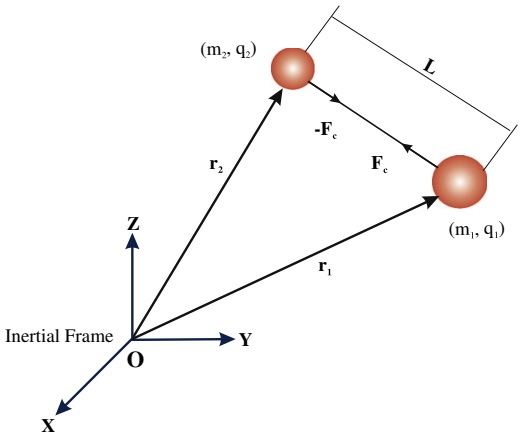

Fig. 1. Two-craft Coulomb spacecraft formation (restricted two-body system).

Using the two-body relative equations of motion with respect to G, the inertial second derivative of the vector $\boldsymbol{r}_g$ is

$$\frac{d^2\boldsymbol{r}_g(t)}{dt^2} + \frac{\mu \boldsymbol{r}_g(t)}{\|\boldsymbol{r}_g(t)\|^3} = 0 \tag{4}$$

where μ is the gravitational constant. Therefore, from Eqs. (2) and (4), the inertial second derivatives of the vectors $\boldsymbol{r}_c$ and $\boldsymbol{r}_g$ are related by

$$\frac{d^2\boldsymbol{r}_c(t)}{dt^2} + \frac{\mu \boldsymbol{r}_g(t)}{\|\boldsymbol{r}_g(t)\|^3} = 0 \tag{5}$$

Let m_1 and m_2 denote the mass of each craft with inertial position vectors $\boldsymbol{r_1}$ and $\boldsymbol{r_2}$, while each craft is assumed to have electrostatic (Coulomb) charges q_1 and q_2. The kinetic energy of the system is then given by

$$T(\dot{\boldsymbol{r}}_1, \dot{\boldsymbol{r}}_2) = \frac{m_1}{2}\|\dot{\boldsymbol{r}}_1\|^2 + \frac{m_2}{2}\|\dot{\boldsymbol{r}}_2\|^2 \tag{6}$$

The potential energy of the system is

$$V(\boldsymbol{r_1}, \boldsymbol{r_2}) = V_g(\boldsymbol{r_1}, \boldsymbol{r_2}) + V_t(\|\boldsymbol{r_1} - \boldsymbol{r_2}\|) \tag{7}$$

where $V_g(\boldsymbol{r_1}, \boldsymbol{r_2})$ is the gravitational potential energy of both the point masses in orbit defined as

$$V_g(\boldsymbol{r_1}, \boldsymbol{r_2}) = -\frac{\mu m_1}{\|\boldsymbol{r_1}\|} - \frac{\mu m_2}{\|\boldsymbol{r_2}\|} \tag{8}$$

$V_t(\|\boldsymbol{r_1} - \boldsymbol{r_2}\|)$ is the elastic tether potential energy and is a function of separation distance $\|\boldsymbol{r_1} - \boldsymbol{r_2}\|$ between the two spacecraft. For example, if a Coulomb tether is assumed between two spacecraft then $V_t = V_c$ with the Coulomb potential energy V_c given by

$$V_c(\|\boldsymbol{r_1} - \boldsymbol{r_2}\|) = k_c \frac{q_1 q_2}{\|\boldsymbol{r_1} - \boldsymbol{r_2}\|} e^{-\|\boldsymbol{r_1} - \boldsymbol{r_2}\|/\lambda_d} \tag{9}$$

where $k_c = 8.9910^9\ \mathrm{Nm}^2/\mathrm{C}^2$ is the Coulomb's constant. The exponential term depends on the Debye length parameter λ_d which controls the electrostatic field strength of plasma shielding between the craft. At Geostationary Orbits (GEO) the Debye length vary between 80 and 1400 m, with a mean of about 180 m [12]. The Coulomb spacecraft formations are typically assumed to be orbiting on high Earth orbits. However, the tether spacecraft formations studied in this paper are assumed to be orbiting from low to high Earth orbits.

In this paper, the relative equilibria of a formation with two spacecraft subjected to elastic tether forces is considered where there are no external forces acting on the system. The relative equilibrium of the spacecraft formation is introduced by defining a uniformly rotating frame located at the origin O which has a constant orbital angular velocity of ξ. A formation moving in a circular orbit that is stationary relative to this uniformly rotating frame exhibits symmetry with respect to the special orthogonal rotation group ***SO***(3). The ***SO***(3) rotation group and other group theoretic concepts used in this paper are briefly explained in Appendix A.

As an example of an elastic tether, a Coulomb formation possesses ***SO***(3) symmetry because both the kinetic and potential energies are invariant under the ***SO***(3) group actions. This ***SO***(3) symmetry reduces the dynamics of the spacecraft formation, and the equilibrium of the reduced dynamics is the relative equilibrium of the formation. If the

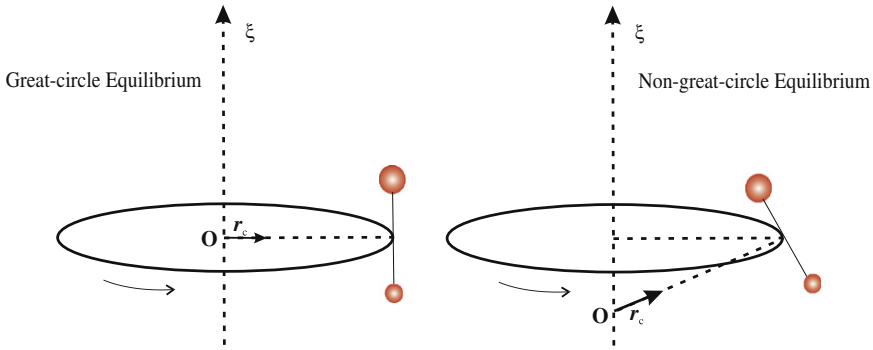

Fig. 2. Two-craft Coulomb spacecraft formation (restricted two-body system).

center of mass of the formation moves on a great-circle orbit, then the relative equilibrium is called the great-circle relative equilibrium. This implies that $\boldsymbol{r}_c \cdot \boldsymbol{\xi} = 0$; if $\boldsymbol{r}_c \cdot \boldsymbol{\xi} \neq 0$ it is called the nongreat-circle relative equilibrium [5] as shown in Fig. 2.

Using the properties of the Lie algebra $\boldsymbol{g}^*$ of $\boldsymbol{SO}(3)$, at relative equilibria there exist two constant inertial vectors $\boldsymbol{r}_{co}$ and $\boldsymbol{r}_{go}$ with respect to O such that $\boldsymbol{r}_c(t) = e^{\hat{\xi}t}\boldsymbol{r}_{co}$ and $\boldsymbol{r}_g(t) = e^{\hat{\xi}t}\boldsymbol{r}_{go}$. Therefore, at relative equilibrium Eq. (5) is reduced to

$$\hat{\xi}\hat{\xi}\boldsymbol{r}_{co} + \frac{\mu \boldsymbol{r}_{go}}{\|\boldsymbol{r}_{go}\|^3} = 0 \tag{10}$$

Taking an inner product of Eq. (10) with ξ gives $\boldsymbol{r}_{go} \cdot \boldsymbol{\xi} = 0$. Consequently, at relative equilibria, the center of gravity of a spacecraft formation moving in a central gravitational field traces a great-circle.

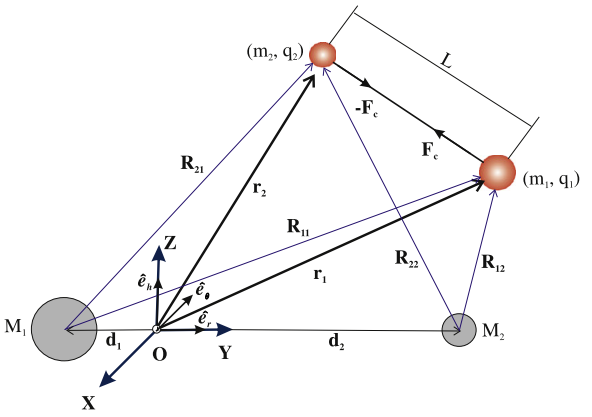

Fig. 3. Two-craft Coulomb spacecraft formation (restricted three-body system).

2.2. Restricted three-body system

In a three-body system, as shown in Fig. 3, the spacecrafts are considered to be point masses moving around the barycenter O under the mutual gravitation of two bodies M_1 and M_2. The relative equilibrium of the spacecraft formation is introduced by defining a uniformly rotating frame located at the barycenter O which has a constant orbital angular velocity of $\boldsymbol{\xi}$. A formation moving in a circular orbit that is stationary relative to this uniformly rotating frame exhibits symmetry with respect to $\boldsymbol{SO}(3)$. If m_1 and m_2 denote the mass of each craft with inertial position vectors $\boldsymbol{R}_{11}$, $\boldsymbol{R}_{12}$, $\boldsymbol{R}_{21}$ and $\boldsymbol{R}_{22}$ then using the three-body relative equations of motion, the inertial second derivative of the vector $\boldsymbol{r}_g$ is

$$M\ddot{\boldsymbol{r}}_g = -\mu_1\left(\frac{m_1}{R_{11}^3}\boldsymbol{R}_{11} + \frac{m_2}{R_{21}^3}\boldsymbol{R}_{21}\right) - \mu_2\left(\frac{m_1}{R_{12}^3}\boldsymbol{R}_{12} + \frac{m_2}{R_{22}^3}\boldsymbol{R}_{22}\right) \tag{11}$$

where M is the total formation mass, and μ_1 and μ_2 are the gravitational parameters of the two planets. The inertial position vectors $\boldsymbol{R}_{11}$, $\boldsymbol{R}_{12}$, $\boldsymbol{R}_{21}$ and $\boldsymbol{R}_{22}$ are expressed in rotating coordinates (synodic frame at the barycenter O) such that the distances are invariant under rotation. The synodic frame $S:\{\hat{\boldsymbol{e}}_r, \hat{\boldsymbol{e}}_\theta, \hat{\boldsymbol{e}}_h\}$ is rotating around the axis Oz with the constant angular velocity Ω defined as

$$\Omega = \sqrt{\frac{G(M_1 + M_2)}{d^3}} \tag{12}$$

where G is the gravity constant and d is the distance between the two planets. The primaries are at rest in the synodic frame at positions $M_1(-d_1,0,0)$ and $M_2(d_2,0,0)$. Also, the kinetic energy of the system is still given by Eq. (6) with rotating position vectors $\boldsymbol{r_1}$ and $\boldsymbol{r_2}$ of the craft. In the potential energy expression in Eq. (7), the elastic tether potential energy remains the same, however, the gravitational potential energy $V_g(\boldsymbol{r_1},\boldsymbol{r_2})$ of the system becomes

$$V_g(\boldsymbol{r_1},\boldsymbol{r_2}) = -\mu_1\left(\frac{m_1}{\|\boldsymbol{r_1}-\boldsymbol{d_1}\|} + \frac{m_2}{\|\boldsymbol{r_2}-\boldsymbol{d_1}\|}\right) - \mu_2\left(\frac{m_1}{\|\boldsymbol{r_1}-\boldsymbol{d_2}\|} + \frac{m_2}{\|\boldsymbol{r_2}-\boldsymbol{d_2}\|}\right) \tag{13}$$

Since the kinetic and potential energy are invariant under $\boldsymbol{SO}(3)$ actions, the elastic tether formation moving around the barycenter has $\boldsymbol{SO}(3)$ symmetry. This symmetry helps in the reduced dynamics by the $\boldsymbol{SO}(3)$ group action and the equilibrium of the reduced dynamics is the relative equilibrium of the spacecraft formation in the three-body system. Therefore, similar to the definitions for a two-body system, in a three-body system $\boldsymbol{r}_c \cdot \boldsymbol{\xi} = 0$ implies that the center of mass of the formation moves on a

great-circle orbit and hence the relative equilibrium is called the great-circle relative equilibrium. And, if $\boldsymbol{r}_c \cdot \boldsymbol{\xi} \neq 0$ it is called the nongreat-circle relative equilibrium. Specifically, the elastic tether is modeled using Coulomb forces and Coulomb tether formations are feasible at Earth–Sun or Earth–Moon Lagrange points [1]. However, in the interplanetary space at a distance of 1 AU from the Sun, the Debye length is much smaller than that in a GEO environment (highest Debye length of approximately 40 m); therefore, this constrains the maximum possible formation length but despite the low value of the Debye length, multi-craft equilibrium formations are reported to exist at the Earth–Sun L1 Lagrange point [17].

3. Relative equilibria of the static two-craft tether formation

Since the static two-craft tether formation possesses $\boldsymbol{SO}(3)$ symmetry, the dynamics in the original phase space of the system is reduced. The relative equilibria of the reduced dynamics facilitates finding the equilibrium configurations. Given a simple mechanical system with symmetry (Q,T,V,G), where Q is the configuration space with G-invariant Riemannian metric K on Q, T is the G-invariant kinetic energy and V is the G-invariant potential function, and G is the symmetry (Lie) group, then we have the following useful theorem based on the principle of symmetric criticality [8].

Theorem. *For a simple dynamical system with symmetry (Q,T,V,G) and the metric*

$$K(\boldsymbol{q})(\boldsymbol{v_q},\boldsymbol{v_q}) = 2T(\boldsymbol{v_q}) \quad \textit{with } \boldsymbol{v_q} \in TQ \tag{14}$$

define the augmented potential $V_\xi : Q \to \mathbf{R}$,

$$V_\xi(\boldsymbol{q}) = V(\boldsymbol{q}) - \frac{1}{2}K(\boldsymbol{q})(\xi_Q(\boldsymbol{q}),\xi_Q(\boldsymbol{q})) \tag{15}$$

where ξ_Q is the infinitesimal generator associated with ξ. Then, at relative equilibrium, $\boldsymbol{q_e}$ is a critical point of V_ξ for some $\xi \in \boldsymbol{g}^*$.

Therefore, for the two-craft tether formation the *augmented* potential function V_ξ is

$$V_\xi(\boldsymbol{r_1},\boldsymbol{r_2}) = V(\boldsymbol{r_1},\boldsymbol{r_2}) - \frac{m_1}{2}\langle \boldsymbol{\xi r_1}, \boldsymbol{\xi r_1} \rangle - \frac{m_2}{2}\langle \boldsymbol{\xi r_2}, \boldsymbol{\xi r_2} \rangle \tag{16}$$

where $\boldsymbol{\xi} \in \mathbf{R}^3$ is an arbitrary constant vector. According to the principle of symmetric criticality, the relative equilibria corresponding to some $\boldsymbol{\xi}$ is characterized by the critical points of the augmented potential V_ξ.

4. Relative equilibria in the restricted two-body system

For the tether spacecraft formation with $\boldsymbol{SO}(3)$ symmetry, the relative equilibrium is one in a uniformly rotating frame. If the vector $\boldsymbol{\xi}$ denotes the angular velocity of the uniformly rotating frame, the augmented potential for the two spacecraft formation is

$$\begin{aligned} V_\xi(\boldsymbol{r_1},\boldsymbol{r_2}) = &-\frac{\mu m_1}{\|\boldsymbol{r_1}\|} - \frac{\mu m_2}{\|\boldsymbol{r_2}\|} + V_t(\|\boldsymbol{r_1}-\boldsymbol{r_2}\|) \\ &- \frac{m_1}{2}\langle \boldsymbol{\xi r_1}, \boldsymbol{\xi r_1} \rangle - \frac{m_2}{2}\langle \boldsymbol{\xi r_2}, \boldsymbol{\xi r_2} \rangle \end{aligned} \tag{17}$$

Then the relative equilibria of the system are characterized by the critical points of the augmented potential V_ξ. The first variation of V_ξ taken component wise with respect to $\boldsymbol{q} = (\boldsymbol{r_1},\boldsymbol{r_2})$ is

$$\begin{aligned} \boldsymbol{D}V_\xi(\boldsymbol{r_1},\boldsymbol{r_2}) \cdot (\delta\boldsymbol{r_1},\delta\boldsymbol{r_2}) = &\mu m_1 \frac{\boldsymbol{r_1}}{\|\boldsymbol{r_1}\|^3} \cdot \delta\boldsymbol{r_1} + \mu m_2 \frac{\boldsymbol{r_2}}{\|\boldsymbol{r_2}\|^3} \cdot \delta\boldsymbol{r_2} \\ &+ V_t'(\|\boldsymbol{r_1}-\boldsymbol{r_2}\|)\frac{\boldsymbol{r_1}-\boldsymbol{r_2}}{\|\boldsymbol{r_1}-\boldsymbol{r_2}\|} \cdot (\delta\boldsymbol{r_1}-\delta\boldsymbol{r_2}) \\ &+ m_1(\hat{\boldsymbol{\xi}}\hat{\boldsymbol{\xi}}\boldsymbol{r_1}) \cdot \delta\boldsymbol{r_1} + m_2(\hat{\boldsymbol{\xi}}\hat{\boldsymbol{\xi}}\boldsymbol{r_2}) \cdot \delta\boldsymbol{r_2} \end{aligned} \tag{18}$$

If $V_t = V_c$, the Coulomb potential, then V_c' denotes the derivative of Coulomb potential with respect to $\|\boldsymbol{r_1}-\boldsymbol{r_2}\|$, which represents the Coulomb force acting between the two crafts. From Eq. (9), V_c' becomes

$$V_c'(\|\boldsymbol{r_1}-\boldsymbol{r_2}\|) = -k_c\frac{q_1 q_2}{\|\boldsymbol{r_1}-\boldsymbol{r_2}\|^2}e^{-\|\boldsymbol{r_1}-\boldsymbol{r_2}\|/\lambda_d}\left[1+\frac{\|\boldsymbol{r_1}-\boldsymbol{r_2}\|}{\lambda_d}\right] \tag{19}$$

Setting $DV_\xi(\boldsymbol{r_{1e}},\boldsymbol{r_{2e}}) = 0$ we arrive at the following conditions of relative equilibria:

$$\frac{\mu m_1 \boldsymbol{r_{1e}}}{r_{1e}^3} + m_1\hat{\boldsymbol{\xi}}\hat{\boldsymbol{\xi}}\boldsymbol{r_{1e}} + V_t'\frac{\boldsymbol{r_{1e}}-\boldsymbol{r_{2e}}}{\|\boldsymbol{r_{1e}}-\boldsymbol{r_{2e}}\|} = 0 \tag{20a}$$

$$\frac{\mu m_2 \boldsymbol{r_{2e}}}{r_{2e}^3} + m_2\hat{\boldsymbol{\xi}}\hat{\boldsymbol{\xi}}\boldsymbol{r_{2e}} - V_t'\frac{\boldsymbol{r_{1e}}-\boldsymbol{r_{2e}}}{\|\boldsymbol{r_{1e}}-\boldsymbol{r_{2e}}\|} = 0 \tag{20b}$$

where $r_{1e} = \|\boldsymbol{r_{1e}}\|$ and $r_{2e} = \|\boldsymbol{r_{2e}}\|$. These equations are valid for any elastic tether type formations and are analogous to those developed in Ref. [8] for a spring-connected system. Therefore, the mathematical development to solve for relative equilibria with line-of-sight elastic forces acting between two spacecraft point masses is similar to that given in Ref. [8].

Now consider a rotation matrix $[RN] \in \boldsymbol{SO}(3)$ that maps vectors from an inertial frame N into a new reference frame R. If we denote the vectors $\boldsymbol{R_1}$, $\boldsymbol{R_2}$, $\boldsymbol{\omega}$ in the reference frame R, then the conditions of relative equilibria given in Eqs. (20) are invariant under the transformation $\boldsymbol{R_1} = [RN]\boldsymbol{r_{1e}}$, $\boldsymbol{R_2} = [RN]\boldsymbol{r_{2e}}$ and $\boldsymbol{\omega} = [RN]\boldsymbol{\xi}$. In order to solve for relative equilibria, the new reference frame should be chosen such that the number of unknowns are at minimum in the equilibrium equations. As illustrated in Fig. 4, a reference frame is chosen such that the x-axis is parallel to the line connecting the two crafts, with the z-axis perpendicular to both the vectors $\boldsymbol{r_{1e}}$ and $\boldsymbol{r_{2e}}$, and the y-axis completing the triad.

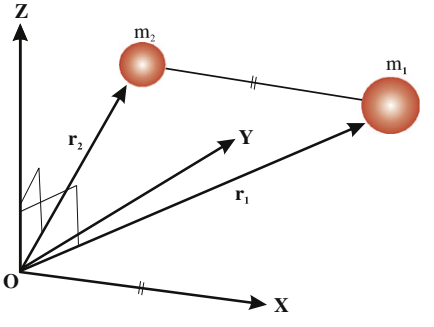

Fig. 4. The rotating reference frame.

In the context of the new frame R, the position vectors are expressed as $\boldsymbol{R}_1=(x_1,y_c,0)^T$, $\boldsymbol{R}_2=(x_2,y_c,0)^T$, and $\boldsymbol{\omega}=(\omega_1,\omega_2,\omega_3)^T$. The equilibrium conditions (20a) and (20b) expressed in scalar form are,

$$-(\omega_2^2+\omega_3^2)x_1+\omega_1\omega_2 y_c+\mu\frac{x_1}{R_1^3}=-\frac{V_t'}{m_1} \tag{21}$$

$$\omega_1\omega_2 x_1-(\omega_1^2+\omega_3^2)y_c+\mu\frac{y_c}{R_1^3}=0 \tag{22}$$

$$(\omega_1 x_1+\omega_2 y_c)\omega_3=0 \tag{23}$$

$$-(\omega_2^2+\omega_3^2)x_2+\omega_1\omega_2 y_c+\mu\frac{x_2}{R_2^3}=\frac{V_t'}{m_2} \tag{24}$$

$$\omega_1\omega_2 x_2-(\omega_1^2+\omega_3^2)y_c+\mu\frac{y_c}{R_2^3}=0 \tag{25}$$

$$(\omega_1 x_2+\omega_2 y_c)\omega_3=0 \tag{26}$$

where $R_1=\|\boldsymbol{R}_1\|$ and $R_2=\|\boldsymbol{R}_2\|$. It is also assumed that $x_1>x_2$ and $L=x_1-x_2>0$. Further, define $\boldsymbol{R}_c=(x_c,y_c,0)^T$ where $x_c=(m_1x_1+m_2x_2)/(m_1+m_2)$. Then the expressions for x_1, x_2 and y_c are

$$x_1=x_c+m_2L/(m_1+m_2) \tag{27a}$$

$$x_2=x_c-m_1L/(m_1+m_2) \tag{27b}$$

$$y_c=\left[R_c^2-\frac{L^2}{4}\left(\frac{m_1-m_2}{m_1+m_2}\right)^2\right]^{1/2} \tag{27c}$$

The relative equilibria of the two-craft formation corresponds to solving the Eqs. (21)–(26) for a given set of values for μ, m_1, m_2, L and $R_c=\|\boldsymbol{R}_c\|$. Ref. [8] presents great-circle and nongreat-circle equilibrium solutions in the context of a spring force acting between two point masses. And these equilibrium results are applicable to any elastic force type such as a Coulomb force acting between the craft. Therefore, such results are utilized to investigate the relative equilibria of elastic tether formation for a range of spacecraft separation distances and semi-major axes. The great-circle and nongreat-circle equilibrium solutions are summarized here and Ref. [8] provides the details of the derivations.

*Case*1a. Setting $\omega_3\neq0$ in the equilibrium conditions and using $y_c\neq0$ yields an *along-track* equilibrium solution (Fig. 5(a))

$$\boldsymbol{R}_1=(1/2L,y_c,0)^T,\quad \boldsymbol{R}_2=(-1/2L,y_c,0)^T,\quad \boldsymbol{\omega}=(0,0,\omega_3)^T$$

$$y_c=R_c,\quad \omega_3^2=\frac{\mu}{R^3}\quad\text{and}\quad V_t'=0.$$

*Case*1b. Setting $\omega_3\neq0$ and $y_c=0$ gives a *radial* equilibrium solution (Fig. 5(b))

$$\boldsymbol{R}_1=(x_1,0,0)^T,\quad \boldsymbol{R}_2=(x_2,0,0)^T,\quad \boldsymbol{\omega}=(0,0,\omega_3)^T$$

$$\omega_3^2=\frac{\mu}{(m_1+m_2)R_c}\left(\frac{m_1}{x_1^2}+\frac{m_2}{x_2^2}\right)\quad\text{and}$$

$$V_t'=\frac{\mu m_1m_2(x_1^3-x_2^3)}{(m_1+m_2)x_1^2x_2^2R_c}>0.$$

*Case*1c. Similarly, $\omega_3=0,y_c\neq0$, and $R_1=R_2$ yields *orbit normal* equilibrium (Fig. 5(c))

$$\boldsymbol{R}_1=(1/2L,y_c,0)^T,\quad \boldsymbol{R}_2=(-1/2L,y_c,0)^T,\quad \boldsymbol{\omega}=(\omega_1,0,0)^T$$

$$m_1=m_2,\quad y_c=R_c,\quad \omega_1^2=\frac{\mu}{R^3},\quad V_t'=-\frac{\mu m_1L}{2R^3}<0$$

*Case*2. Setting $\omega_3=0,y_c\neq0,R_1\neq R_2$ gives *nongreat-circle* equilibrium solution (Fig. 5(d)) As in Ref. [8], manipulating Eqs. (21)–(26) yields the condition $x_c\omega_1+y_c\omega_2\neq0$, or equivalently, $\boldsymbol{R}_c\cdot\boldsymbol{\omega}\neq0$. This analytically proves that for the given conditions in Case 2 there is no great-circle

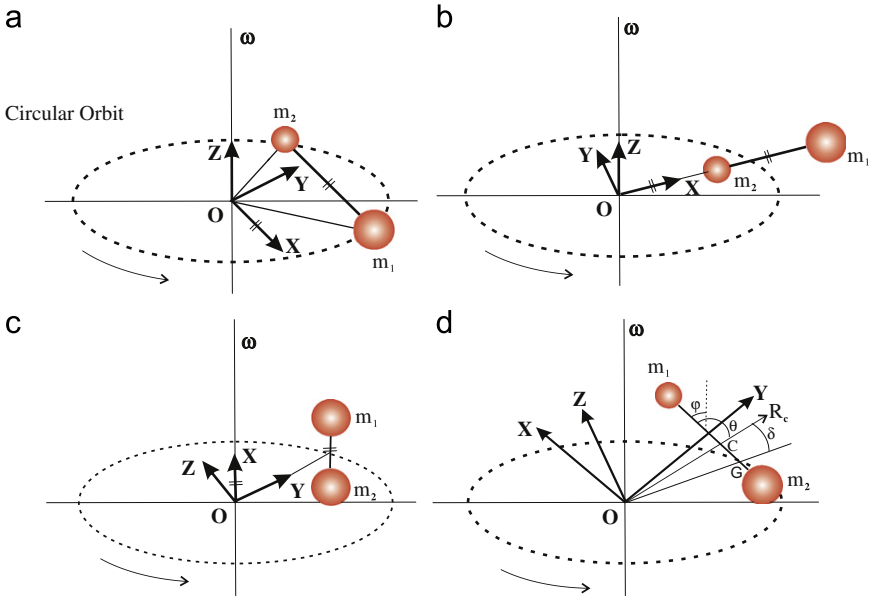

Fig. 5. Relative equilibrium solutions: (a) tangential, (b) radial, (c) orbit normal and (d) non-great-circle.

equilibria. Additionally, Ref. [8] shows that nongreat-circle equilibria exist only if $m_1 \neq m_2$. For instance, Coulomb formations allow very lumpy distribution of masses and thus, these nongreat-circle equilibria conditions are of interest. Therefore, the nongreat-circle equilibrium conditions are

$$\boldsymbol{R}_1 = (x_1, y_c, 0)^T, \quad \boldsymbol{R}_2 = (x_2, y_c, 0)^T, \quad \boldsymbol{\omega} = (\omega_1, \omega_2, 0)^T \tag{28}$$

and

$$f = f_x f_1 + f_y f_2 = 0 \tag{29}$$

where

$$f_x = \frac{m_1 x_1}{R_1^3} + \frac{m_2 x_2}{R_2^3}$$

$$f_1 = \frac{x_2}{R_1^3} - \frac{x_1}{R_2^3}$$

$$f_y = \left(\frac{m_1}{R_1^3} + \frac{m_2}{R_2^3}\right) y_c$$

$$f_2 = \left(\frac{1}{R_1^3} - \frac{1}{R_2^3}\right) y_c$$

Therefore, f written in terms of m_1, m_2, R_1, R_2, x_c, y_c and L is

$$f = \left(x_c^2 + y_c^2 - \frac{L^2 m_1 m_2}{(m_1+m_2)^2}\right)\left(\frac{m_1}{R_1^6} + \frac{m_2 - m_1}{R_1^3 R_2^3} - \frac{m_2}{R_2^6}\right) + \frac{x_c L}{m_1+m_2}\left((m_2-m_1)\left(\frac{m_1}{R_1^6} - \frac{m_2}{R_2^6}\right) - \frac{4 m_1 m_2}{R_1^3 R_2^3}\right) = 0 \tag{30}$$

The solutions of Eq. (30) provide the nongreat-circle equilibria. This formulation of the nongreat-circle equilibria is independent of tether force between the spacecraft and is thus useful for analyzing the equilibria for a range of spacecraft separation distances from LEO to GEO heights. In order to simplify the solution methodology, Eq. (30) is expressed in terms of one variable θ, the angle between $\boldsymbol{R}_c$ and the x-axis of the rotating frame as shown in Fig. 5(d). Therefore, let $x_c = R_c \cos(\theta)$ and $y_c = R_c \sin(\theta)$. Plugging in these x_c and y_c values into Eq. (30) yields a function of θ for given values of μ, m_1, m_2, L and R_c. Since $f(\theta)$ is a continuous function for a tether formation on $[0,\pi]$, with $(R_c \gg L)$ and $f(0) < 0$, $f(\pi) > 0$, there exists at least one solution for $f(\theta) = 0$. Furthermore, since $df(\theta)/d\theta > 0$ on $[0,\pi]$, this solution is unique. The actual deflection angle, ϕ, from the vertical is computed from the angle between x-axis and $\boldsymbol{\omega}$, while $\theta - \phi$ is the angle between $\boldsymbol{\omega}$ and $\boldsymbol{R}_c$. The deflection angle ϕ and error δ are shown in Fig. 5(d) where the error δ is defined to be $\theta - \phi - 90$.

Table 1
Nongreat-circle relative equilibria at LEO [8].

m_1 (kg)	m_2 (kg)	θ (deg)	ϕ (deg)	δ (deg)
100	9900	91.052659	1.052684	−0.000026048

Ref. [8] discusses the existence of nongreat-circle equilibria for long tethers. For spacecraft that are separated by 350 km at LEO a deflection of about 1 from the vertical to the orbital plane is observed. For instance, Table 1 shows the results of $f(\theta) = 0$ for LEO where $R_c = 7000$ km and $L = 350$ km. The error $\delta \neq 0$ numerically proves the existence of nongreat-circle equilibria for long tethers. To gain further insights, the effect of nongreat-circle equilibria on a two-craft formation is studied as a function of spacecraft separation distance L and mass distribution ratio χ defined as

$$\chi = \frac{m_1}{m_1 + m_2} \tag{31}$$

The spacecraft separation distances range from 10 m to 1000 km and formation center of mass distances from LEO to GEO heights. The contour plots shown in Fig. 6 indicate that increasing the semi-major axes R_c while holding L fixed leads to a decrease in deflection. However, fixing R_c and allowing L to increase leads to an increase in deflections. As the spacecraft formation becomes more asymmetric, the contour plots show that as spacecraft separation distances L reach 1000 km, deflections of up to the order of 10 are observed. Therefore, large separation distances and mass asymmetry has an effect at LEO to GEO heights; however, for tether formation separation distances on the order of hundreds of meters, the deflection from normal is less than 10^{-6} degrees, and mass asymmetry also showed negligible effect on the attitude deflection. Even for a case where there is a 1:10,000 mass ratio, the nongreat-circle equilibria deflection from low earth orbits to geostationary orbits is less than 10^{-5} degrees. Evaluating Eq. (30) yields very small function values (on the order of 10^{-12}) and hence the solutions are limited to a lower bound of 10^{-6} degrees. This numerically unresolved region is shown as "noise" pattern in Fig. 6. However, this degree of accuracy is sufficient to ignore the effect of orbit-attitude coupling for short tether formation separation distances. Specifically, for Coulomb formation separation distances on the order of dozens of meters at GEO, thus ignoring orbit-attitude coupling, the use of numerical search algorithms such as evolutionary search strategies is justified in the search for static Coulomb structures.

5. Relative equilibria in the restricted three-body system

In a restricted three-body system for the Coulomb spacecraft formation with ***SO***(3) symmetry, the relative equilibrium is one in a uniformly rotating frame. If the vector $\boldsymbol{\xi}$ denotes the angular velocity of the uniformly rotating frame located at barycenter O, the augmented potential for the two spacecraft formation is

$$V_\xi(\boldsymbol{r_1}, \boldsymbol{r_2}) = -\mu_1\left(\frac{m_1}{\|\boldsymbol{r_1} - \boldsymbol{d_1}\|} + \frac{m_2}{\|\boldsymbol{r_2} - \boldsymbol{d_1}\|}\right) - \mu_2\left(\frac{m_1}{\|\boldsymbol{r_1} - \boldsymbol{d_2}\|} + \frac{m_2}{\|\boldsymbol{r_2} - \boldsymbol{d_2}\|}\right) + V_t(\|\boldsymbol{r_1} - \boldsymbol{r_2}\|) - \frac{m_1}{2}\langle \boldsymbol{\xi r_1}, \boldsymbol{\xi r_1} \rangle - \frac{m_2}{2}\langle \boldsymbol{\xi r_2}, \boldsymbol{\xi r_2} \rangle \tag{32}$$

In this case, the relative equilibria of the system are characterized by the critical points of the augmented potential V_ξ. The first variation of V_ξ taken component

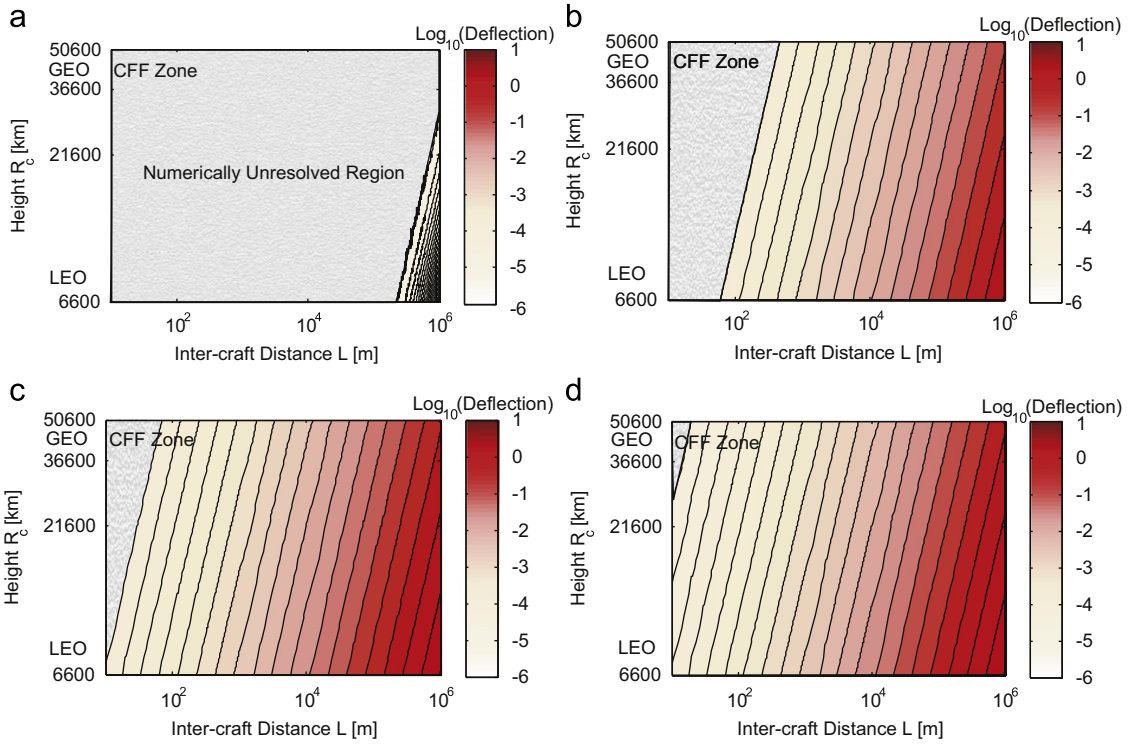

Fig. 6. Deflection for an asymmetric mass distribution (deg). (a) $\chi = 0.49975$, (b) $\chi = 0.35$, (c) $\chi = 0.05$, (d) $\chi = 0.0001$.

wise with respect to $\boldsymbol{q} = (\boldsymbol{r_1}, \boldsymbol{r_2})$ is

$$
\begin{aligned}
&\boldsymbol{D}V_{\xi}(\boldsymbol{r_1},\boldsymbol{r_2})\cdot(\delta\boldsymbol{r_1},\delta\boldsymbol{r_2}) \\
&\quad = \mu_1 m_1 \frac{\boldsymbol{r_1}-\boldsymbol{d_1}}{\|\boldsymbol{r_1}-\boldsymbol{d_1}\|^3}\cdot\delta\boldsymbol{r_1} + \mu_1 m_2 \frac{\boldsymbol{r_2}-\boldsymbol{d_1}}{\|\boldsymbol{r_2}-\boldsymbol{d_1}\|^3}\cdot\delta\boldsymbol{r_2} \\
&\quad + \mu_2 m_1 \frac{\boldsymbol{r_1}-\boldsymbol{d_2}}{\|\boldsymbol{r_1}-\boldsymbol{d_2}\|^3}\cdot\delta\boldsymbol{r_1} + \mu_2 m_2 \frac{\boldsymbol{r_2}-\boldsymbol{d_2}}{\|\boldsymbol{r_2}-\boldsymbol{d_2}\|^3}\cdot\delta\boldsymbol{r_2} \\
&\quad + V_t'(\|\boldsymbol{r_1}-\boldsymbol{r_2}\|)\frac{\boldsymbol{r_1}-\boldsymbol{r_2}}{\|\boldsymbol{r_1}-\boldsymbol{r_2}\|}\cdot(\delta\boldsymbol{r_1}-\delta\boldsymbol{r_2}) \\
&\quad + m_1(\hat{\boldsymbol{\xi}}\hat{\boldsymbol{\xi}}\boldsymbol{r_1})\cdot\delta\boldsymbol{r_1} + m_2(\hat{\boldsymbol{\xi}}\hat{\boldsymbol{\xi}}\boldsymbol{r_2})\cdot\delta\boldsymbol{r_2}
\end{aligned} \tag{33}
$$

If $V_t = V_c$, the Coulomb potential, then V_c' is given by Eq. (19). Setting $DV_{\xi}(\boldsymbol{r_{1e}},\boldsymbol{r_{2e}}) = 0$ leads to the following relative equilibria conditions:

$$
\mu_1 m_1 \frac{\boldsymbol{r_{1e}}-\boldsymbol{d_1}}{\|\boldsymbol{r_{1e}}-\boldsymbol{d_1}\|^3} + \mu_2 m_1 \frac{\boldsymbol{r_{1e}}-\boldsymbol{d_2}}{\|\boldsymbol{r_{1e}}-\boldsymbol{d_2}\|^3} + m_1\hat{\boldsymbol{\xi}}\hat{\boldsymbol{\xi}}\boldsymbol{r_{1e}} + V_t'\frac{\boldsymbol{r_{1e}}-\boldsymbol{r_{2e}}}{\|\boldsymbol{r_{1e}}-\boldsymbol{r_{2e}}\|} = 0 \tag{34a}
$$

$$
\mu_1 m_2 \frac{\boldsymbol{r_{2e}}-\boldsymbol{d_1}}{\|\boldsymbol{r_{2e}}-\boldsymbol{d_1}\|^3} + \mu_2 m_2 \frac{\boldsymbol{r_{2e}}-\boldsymbol{d_2}}{\|\boldsymbol{r_{2e}}-\boldsymbol{d_2}\|^3} + m_2\hat{\boldsymbol{\xi}}\hat{\boldsymbol{\xi}}\boldsymbol{r_{2e}} - V_t'\frac{\boldsymbol{r_{1e}}-\boldsymbol{r_{2e}}}{\|\boldsymbol{r_{1e}}-\boldsymbol{r_{2e}}\|} = 0 \tag{34b}
$$

The vectors $\boldsymbol{R}_{11}$, $\boldsymbol{R}_{12}$, $\boldsymbol{R}_{21}$ and $\boldsymbol{R}_{22}$ shown in Fig. 3 are represented in terms of $\boldsymbol{r_{1e}}$, $\boldsymbol{r_{2e}}$, $\boldsymbol{d}_1$, and $\boldsymbol{d}_2$ as

$$
\begin{aligned}
&\boldsymbol{R}_{11} = \boldsymbol{r_{1e}}-\boldsymbol{d}_1, \quad \boldsymbol{R}_{12} = \boldsymbol{r_{1e}}-\boldsymbol{d}_2 \\
&\boldsymbol{R}_{21} = \boldsymbol{r_{2e}}-\boldsymbol{d}_1, \quad \boldsymbol{R}_{22} = \boldsymbol{r_{2e}}-\boldsymbol{d}_2
\end{aligned} \tag{35}
$$

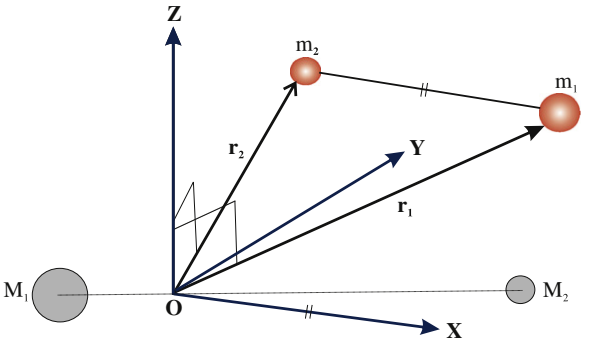

Fig. 7. The rotating reference frame (restricted three-body system).

Therefore, Eqs. (34a) and (34b) become

$$
\mu_1 m_1 \frac{\boldsymbol{r_{1e}}-\boldsymbol{d_1}}{\boldsymbol{R}_{11}^3} + \mu_2 m_1 \frac{\boldsymbol{r_{1e}}-\boldsymbol{d_2}}{\boldsymbol{R}_{12}^3} + m_1\hat{\boldsymbol{\xi}}\hat{\boldsymbol{\xi}}\boldsymbol{r_{1e}} + V_t'\frac{\boldsymbol{r_{1e}}-\boldsymbol{r_{2e}}}{\|\boldsymbol{r_{1e}}-\boldsymbol{r_{2e}}\|} = 0 \tag{36a}
$$

$$
\mu_1 m_2 \frac{\boldsymbol{r_{2e}}-\boldsymbol{d_1}}{\boldsymbol{R}_{21}^3} + \mu_2 m_2 \frac{\boldsymbol{r_{2e}}-\boldsymbol{d_2}}{\boldsymbol{R}_{22}^3} + m_2\hat{\boldsymbol{\xi}}\hat{\boldsymbol{\xi}}\boldsymbol{r_{2e}} - V_t'\frac{\boldsymbol{r_{1e}}-\boldsymbol{r_{2e}}}{\|\boldsymbol{r_{1e}}-\boldsymbol{r_{2e}}\|} = 0 \tag{36b}
$$

where $R_{11} = \|\boldsymbol{R}_{11}\|$, $R_{12} = \|\boldsymbol{R}_{12}\|$, $R_{21} = \|\boldsymbol{R}_{21}\|$ and $R_{22} = \|\boldsymbol{R}_{22}\|$.

Now consider a rotation matrix $[FS] \in \boldsymbol{SO}(3)$ that maps vectors from a synodic frame S into a new reference frame F. If we denote the vectors $\boldsymbol{R_1}$, $\boldsymbol{R_2}$, $\boldsymbol{\omega}$ in the reference frame S, then the conditions of relative equilibria given in

Eqs. (36) are invariant under the transformation $\boldsymbol{R_1}=[FS]\boldsymbol{r_{1e}}$, $\boldsymbol{R_2}=[FS]\boldsymbol{r_{2e}}$ and $\boldsymbol{\omega}=[FS]\boldsymbol{\xi}$. As illustrated in Fig. 7, a reference frame is chosen such that the x-axis is parallel to the line connecting the two crafts, the z-axis being perpendicular to both the vectors $\boldsymbol{r_{1e}}$ and $\boldsymbol{r_{2e}}$, and the y-axis completing the triad. Also, let γ be the angle in the orbit plane between the two frames S and F.

In the context of the new frame F, the position vectors are expressed as $\boldsymbol{R}_1=(x_1,y_c,0)^T$, $\boldsymbol{R}_2=(x_2,y_c,0)^T$, and $\boldsymbol{\omega}=(\omega_1,\omega_2,\omega_3)^T$. The vectors $\boldsymbol{d}_1$ and $\boldsymbol{d}_2$ in the F frame become $(-d_1\cos\gamma,-d_1\sin\gamma,0)$ and $(d_2\cos\gamma,d_2\sin\gamma,0)$. Now the equilibrium conditions (36a) and (36b) expressed in scalar form are

$$-(\omega_2^2+\omega_3^2)x_1+\omega_1\omega_2y_c+\mu_1\left(\frac{x_1+d_1\cos\gamma}{R_{11}^3}\right)+\mu_2\left(\frac{x_1-d_2\cos\gamma}{R_{12}^3}\right)=-\frac{V_t'}{m_1} \tag{37}$$

$$\omega_1\omega_2x_1-(\omega_1^2+\omega_3^2)y_c+\mu_1\left(\frac{y_c+d_1\sin\gamma}{R_{11}^3}\right)+\mu_2\left(\frac{y_c-d_2\sin\gamma}{R_{12}^3}\right)=0 \tag{38}$$

$$(\omega_1x_1+\omega_2y_c)\omega_3=0 \tag{39}$$

$$-(\omega_2^2+\omega_3^2)x_2+\omega_1\omega_2y_c+\mu_1\left(\frac{x_2+d_1\cos\gamma}{R_{21}^3}\right)+\mu_2\left(\frac{x_2-d_2\cos\gamma}{R_{22}^3}\right)=\frac{V_t'}{m_2} \tag{40}$$

$$\omega_1\omega_2x_2-(\omega_1^2+\omega_3^2)y_c+\mu_1\left(\frac{y_c+d_1\sin\gamma}{R_{21}^3}\right)+\mu_2\left(\frac{y_c-d_2\sin\gamma}{R_{22}^3}\right)=0 \tag{41}$$

$$(\omega_1x_2+\omega_2y_c)\omega_3=0 \tag{42}$$

It is also assumed that $x_1>x_2$ and let $L=x_1-x_2>0$. Further, define $\boldsymbol{R}_c=(x_c,y_c,0)^T$ where $x_c=(m_1x_1+m_2x_2)\ /(m_1+m_2)$. The expressions for x_1, x_2 and y_c are given in Eq. (27c).

Determining the relative equilibria of the two-craft formation corresponds to solving the Eqs. (37–42) for a given set of values for μ_1, μ_2, m_1, m_2, L and $R_c=\|\boldsymbol{R}_c\|$. Since there are more unknowns than the number of equations, certain constraints are needed in order to find the relative equilibria. For libration point missions, the frame rotates at a constant angular velocity Ω given in Eq. (12). Let us consider angular velocity constraints $\omega_3=\Omega\neq0$ (Case 1) and $\omega_3=0$ (Case 2).

*Case*1. As $\omega_3\neq0$ Eq. (39) implies $(\omega_1x_1+\omega_2y_c)=0$ and $x_1\neq0$ due to the adopted frame which indicates that $\omega_1=0$ and $\omega_2y_c=0$. Using the conditions $\omega_3\neq0$ and $\omega_1=0$ in Eqs. (38) and (41) and subtracting one from the other gives rise to

$$\left[\mu_1\left(\frac{1}{R_{11}^3}-\frac{1}{R_{21}^3}\right)(y_c+d_1\sin\gamma)+\mu_2\left(\frac{1}{R_{12}^3}-\frac{1}{R_{22}^3}\right)(y_c-d_2\sin\gamma)\right]=0 \tag{43}$$

From Eq. (43), two more conditions arise, $y_c+d_1\sin\gamma\neq0$ and $y_c-d_2\sin\gamma\neq0$, or $y_c+d_1\sin\gamma=0$ and $y_c-d_2\sin\gamma=0$. Therefore, the conditions for relative equilibria are further expressed as Cases 1a and 1b.

*Case*1a. $\omega_1=0$, $\omega_3\neq0$, $\omega_2y_c=0$, $y_c+d_1\sin\gamma\neq0$ and $y_c-d_2\sin\gamma\neq0$.

Here, $y_c+d_1\sin\gamma\neq0$ implies that $y_c\neq0$ and $\gamma\neq0$. This forces $\omega_2=0$ and Eq. (43) yields $R_{11}=R_{21}$ and $R_{12}=R_{22}$. Applying these conditions to Eqs. (37) and (40) and dividing by the other results in the conditions $(m_1x_1+m_2x_2)=0$ and $\gamma=90$. Therefore, the *along-track* equilibrium solutions in the context of a restricted three-body system (circular orbits) are

$$\boldsymbol{R}_1=\left(\frac{1}{2}L,y_c,0\right)^T,\quad \boldsymbol{R}_2=\left(-\frac{1}{2}L,y_c,0\right)^T,\quad \boldsymbol{\omega}=(0,0,\Omega)^T$$

$$y_c=R_c,\quad \text{and}\quad V_t'=-\frac{m_1m_2L}{(m_1+m_2)}\left(\left(\frac{\mu_1}{R_{11}^3}+\frac{\mu_2}{R_{12}^3}\right)-\Omega^2\right)$$

Since $\boldsymbol{R}_c\cdot\boldsymbol{\omega}=0$, this is a great-circle relative equilibrium. However, in the context of a restricted three-body system, for any of the collinear libration points it can be shown that $\Omega^2<\mu_1/R_{11}^3+\mu_2/R_{12}^3$, which implies that $V_t'<0$ (compressive elastic force). For any of the triangular libration points it can be shown that $\Omega^2>\mu_1/R_{11}^3+\mu_2/R_{12}^3$, which implies that $V_t'>0$ (tensile elastic force). For example, Fig. 8 shows the along-track equilibrium solutions at a collinear (L_2) and a triangular (L_4) libration point. In particular, for a Coulomb tether, Eq. (19) indicates that the two spacecraft masses must be charged with same polarity at the collinear libration points and must be charged with opposite polarity at the triangular libration points.

*Case*1b. $\omega_1=0$, $\omega_3=\Omega\neq0$, $\omega_2y_c=0$, $y_c+d_1\sin\gamma=0$ and $y_c-d_2\sin\gamma=0$.

Assuming that $x_1>x_2>0$ for a tether formation and since $\omega_3\neq0$ and $y_c+d_1\sin\gamma=0$,$y_c-d_2\sin\gamma=0$ implies that $y_c=0$ and $\gamma=0$ for collinear libration points. However, for Earth–Moon triangular libration points $y_c=0$ and $\gamma=60.31$, appropriate values of R_{11}, R_{12}, R_{21} and R_{22} should satisfy Eq. (43). Therefore, for any libration point, from Eq. (39) one can set $\omega_1=0$ and $\omega_2=0$. With these conditions, Eqs. (37)–(42) reduce to

$$\left(-\Omega^2+\frac{\mu_1}{R_{11}^3}+\frac{\mu_2}{R_{12}^3}\right)x_1+\frac{\mu_1d_1}{R_{11}^3}-\frac{\mu_2d_2}{R_{12}^3}=-\frac{V_t'}{m_1} \tag{44a}$$

$$\left(-\Omega^2+\frac{\mu_1}{R_{21}^3}+\frac{\mu_2}{R_{22}^3}\right)x_2+\frac{\mu_1d_1}{R_{21}^3}-\frac{\mu_2d_2}{R_{22}^3}=\frac{V_t'}{m_2} \tag{44b}$$

Solving these equations yields a *radial* relative equilibrium with the tether forces directed along the radial axis. The equilibrium solution configuration is

$$\boldsymbol{R}_1=(x_1,0,0)^T,\quad \boldsymbol{R}_2=(x_2,0,0)^T,\quad \boldsymbol{\omega}=(0,0,\Omega)^T$$

$$V_t'=\frac{m_1m_2}{m_1+m_2}\left(\Omega^2L-\mu_1\left(\frac{1}{R_{11}^3}-\frac{1}{R_{21}^3}\right)-\mu_2\left(\frac{1}{R_{12}^3}-\frac{1}{R_{22}^3}\right)\right)$$

Since $x_1>x_2$, from Eq. (35) it can be shown for a radial equilibrium that $R_{11}>R_{21}$ and $R_{12}>R_{22}$ for both the collinear and triangular libration points, indicating that

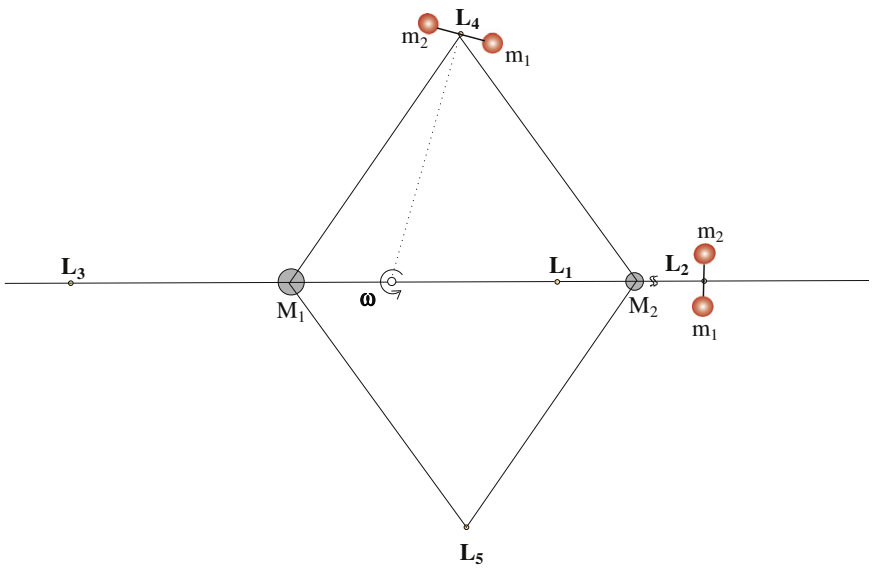

Fig. 8. Along-track relative equilibrium.

$V_t' > 0$. Again, $\boldsymbol{R}_c \cdot \boldsymbol{\omega} = 0$ is a great-circle relative equilibrium as shown in Fig. 9. This implies that there is a tensile elastic force acting between the two masses along the radial direction when the formation is at any of the libration points. Hence, for a Coulomb tether, $V_t' > 0$ indicates that the two spacecraft masses must be charged with opposite polarity.

*Case*2. $\omega_3 = 0$. The relative equilibrium equations reduce to

$$-\omega_2^2 x_1 + \omega_1\omega_2 y_c + \mu_1\left(\frac{x_1 + d_1\cos\gamma}{R_{11}^3}\right) + \mu_2\left(\frac{x_1 - d_2\cos\gamma}{R_{12}^3}\right) = -\frac{V_t'}{m_1} \tag{45a}$$

$$\omega_1\omega_2 x_1 - \omega_1^2 y_c + \mu_1\left(\frac{y_c + d_1\sin\gamma}{R_{11}^3}\right) + \mu_2\left(\frac{y_c - d_2\sin\gamma}{R_{12}^3}\right) = 0 \tag{45b}$$

$$-\omega_2^2 x_2 + \omega_1\omega_2 y_c + \mu_1\left(\frac{x_2 + d_1\cos\gamma}{R_{21}^3}\right) + \mu_2\left(\frac{x_2 - d_2\cos\gamma}{R_{22}^3}\right) = \frac{V_t'}{m_2} \tag{45c}$$

$$\omega_1\omega_2 x_2 - \omega_1^2 y_c + \mu_1\left(\frac{y_c + d_1\sin\gamma}{R_{21}^3}\right) + \mu_2\left(\frac{y_c - d_2\sin\gamma}{R_{22}^3}\right) = 0 \tag{45d}$$

Setting $y_c + d_1\sin\gamma = 0$ and $y_c - d_2\sin\gamma = 0$, the equilibrium conditions yield radial equilibrium solutions as seen in Case 1b, but with ω_3 replaced by ω_2. Therefore, we consider only the case where $y_c + d_1\sin\gamma \neq 0$ and $y_c - d_2\sin\gamma \neq 0$. Furthermore, it is assumed that $R_{11} = R_{21}$ and $R_{12} = R_{22}$ (Case 2a) as well as $R_{11} \neq R_{21}$ and $R_{12} \neq R_{22}$ (Case 2b).

*Case*2a. $\omega_3 = 0$, $R_{11} = R_{21}$, $R_{12} = R_{22}$, $y_c + d_1\sin\gamma \neq 0$ and $y_c - d_2\sin\gamma \neq 0$.

Using $y_c + d_1\sin\gamma \neq 0$ and $y_c - d_2\sin\gamma \neq 0$ yields $R_{11} = R_{21}$ and $R_{12} = R_{22}$, giving the condition $x_1 = -x_2$. Eqs. (45b) and (45d) imply that $\omega_1 \neq 0$; additionally, set $\omega_1 = \Omega$ and $\omega_2 = 0$. Then, using $x_1 = -x_2$ and $\omega_2 = 0$ in Eqs. (45a) and (45c) yields $m_1 = m_2$ as the only possible condition. As a result, the equilibrium solutions obtained are

$$\boldsymbol{R}_1 = \left(\frac{1}{2}L, y_c, 0\right)^T, \quad \boldsymbol{R}_2 = \left(-\frac{1}{2}L, y_c, 0\right)^T, \quad \boldsymbol{\omega} = (\Omega, 0, 0)^T$$

$$m_1 = m_2, \quad y_c = R_c, \quad V_t' = -\frac{m_1 m_2 L}{(m_1 + m_2)}\left(\frac{\mu_1}{R_{11}^3} + \frac{\mu_2}{R_{12}^3}\right) < 0$$

These *orbit normal* equilibrium solutions are applicable for both triangular and collinear libration points. Specifically, for triangular libration points $R_{11} = R_{21} = R_{12} = R_{22}$ holds true. Since $\boldsymbol{R}_c \cdot \boldsymbol{\omega} = 0$, once again this is a great-circle relative equilibrium. Since $V_t' < 0$, there is a compressive elastic force acting between the two masses perpendicular to the orbital plane and the two masses are equal and equidistant from the barycenter. Fig. 10 specifically, illustrates this for a collinear (L_2) and a triangular (L_4) libration point. For a Coulomb formation, since $V_c' < 0$, the two spacecraft masses must be charged with the same polarity.

*Case*2b. $\omega_3 = 0$, $R_{11} \neq R_{21}$, $R_{12} \neq R_{22}$, $y_c + d_1\sin\gamma \neq 0$ and $y_c - d_2\sin\gamma \neq 0$.

Assuming that the F frame is aligned with the orbit normal configuration gives $\gamma = 90$. Solving Eqs. (45b) and (45d) yields

$$-(x_1 - x_2)\omega_1\omega_2 = y_c\left(\left(\frac{\mu_1}{R_{11}^3} + \frac{\mu_2}{R_{12}^3}\right) - \left(\frac{\mu_1}{R_{21}^3} + \frac{\mu_2}{R_{22}^3}\right)\right) + \mu_1 d_1\left(\frac{1}{R_{11}^3} - \frac{1}{R_{21}^3}\right) + \mu_2 d_2\left(\frac{1}{R_{22}^3} - \frac{1}{R_{12}^3}\right) \neq 0 \tag{46}$$

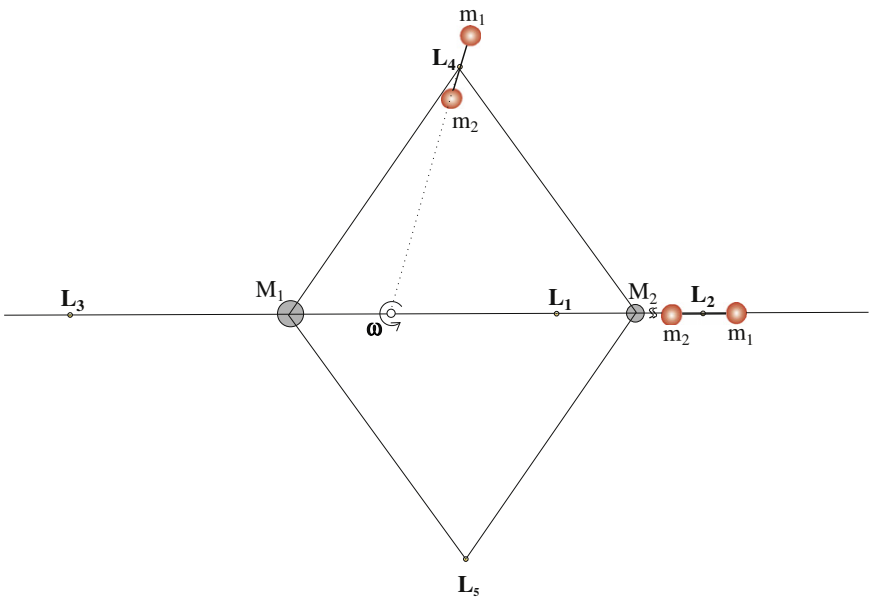

Fig. 9. Radial relative equilibrium.

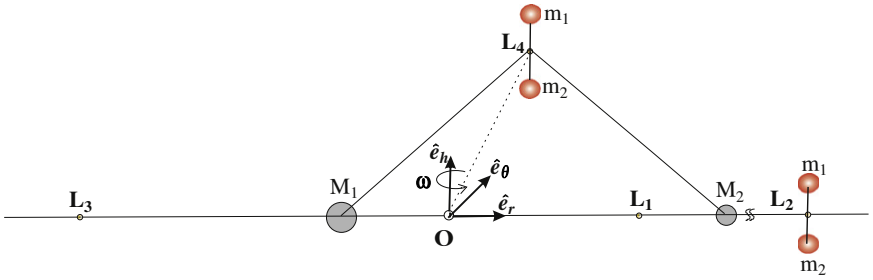

Fig. 10. Orbit normal relative equilibrium.

which implies that $\omega_1 \neq 0$ and $\omega_2 \neq 0$. Combining Eqs. (45a) and (45c)

$$(m_1+m_2)(\omega_2 x_c - \omega_1 y_c)\omega_2 = m_1 x_1\left(\frac{\mu_1}{R_{11}^3}+\frac{\mu_2}{R_{12}^3}\right)+m_2 x_2\left(\frac{\mu_1}{R_{21}^3}+\frac{\mu_2}{R_{22}^3}\right)\neq 0 \tag{47}$$

Eq. (47) implies that $(\omega_2 x_c - \omega_1 y_c)\neq 0$. Multiplying Eq. (45b) by m_1 and (45d) by m_2 and adding the resulting equations gives

$$-(m_1+m_2)(\omega_2 x_c-\omega_1 y_c)\omega_1 = \left(m_1\left(\frac{\mu_1}{R_{11}^3}+\frac{\mu_2}{R_{12}^3}\right)+m_2\left(\frac{\mu_1}{R_{21}^3}+\frac{\mu_2}{R_{22}^3}\right)\right)y_c + m_1\left(\frac{\mu_1 d_1}{R_{11}^3}-\frac{\mu_2 d_2}{R_{12}^3}\right)+m_2\left(\frac{\mu_1 d_1}{R_{21}^3}-\frac{\mu_2 d_2}{R_{22}^3}\right)\neq 0 \tag{48}$$

Defining f_x and f_y to be

$$f_x = \mu_1\left(\frac{m_1 x_1}{R_{11}^3}+\frac{m_2 x_2}{R_{21}^3}\right)+\mu_2\left(\frac{m_1 x_1}{R_{12}^3}+\frac{m_2 x_2}{R_{22}^3}\right)\neq 0 \tag{49}$$

$$f_y = \left(\mu_1\left(\frac{m_1}{R_{11}^3}+\frac{m_2}{R_{21}^3}\right)+\mu_2\left(\frac{m_1}{R_{12}^3}+\frac{m_2}{R_{22}^3}\right)\right)y_c + m_1\left(\frac{\mu_1 d_1}{R_{11}^3}-\frac{\mu_2 d_2}{R_{12}^3}\right)+m_2\left(\frac{\mu_1 d_1}{R_{21}^3}-\frac{\mu_2 d_2}{R_{22}^3}\right)\neq 0 \tag{50}$$

The ratio of Eqs. (47) and (48) becomes

$$\frac{\omega_2}{\omega_1} = -\frac{f_x}{f_y} \tag{51}$$

Eliminating ω_1 and ω_2 from Eqs. (46)–(48) yields

$$f = f_x f_1 + f_y f_2 = 0 \tag{52}$$

where

$$f_1 = x_2\left(\frac{\mu_1}{R_{11}^3}+\frac{\mu_2}{R_{12}^3}\right)-x_1\left(\frac{\mu_1}{R_{21}^3}+\frac{\mu_2}{R_{22}^3}\right)+\left(x_2\left(\frac{\mu_1 d_1}{R_{11}^3}-\frac{\mu_2 d_2}{R_{12}^3}\right)+x_1\left(\frac{\mu_2 d_2}{R_{22}^3}-\frac{\mu_1 d_1}{R_{21}^3}\right)\right)\frac{1}{y_c}$$

and

$$f_2 = \left(\left(\frac{\mu_1}{R_{11}^3}+\frac{\mu_2}{R_{12}^3}\right)-\left(\frac{\mu_1}{R_{21}^3}+\frac{\mu_2}{R_{22}^3}\right)\right)y_c+\left(\frac{\mu_1 d_1}{R_{11}^3}-\frac{\mu_2 d_2}{R_{12}^3}\right)+\left(\frac{\mu_2 d_2}{R_{22}^3}-\frac{\mu_1 d_1}{R_{21}^3}\right)$$

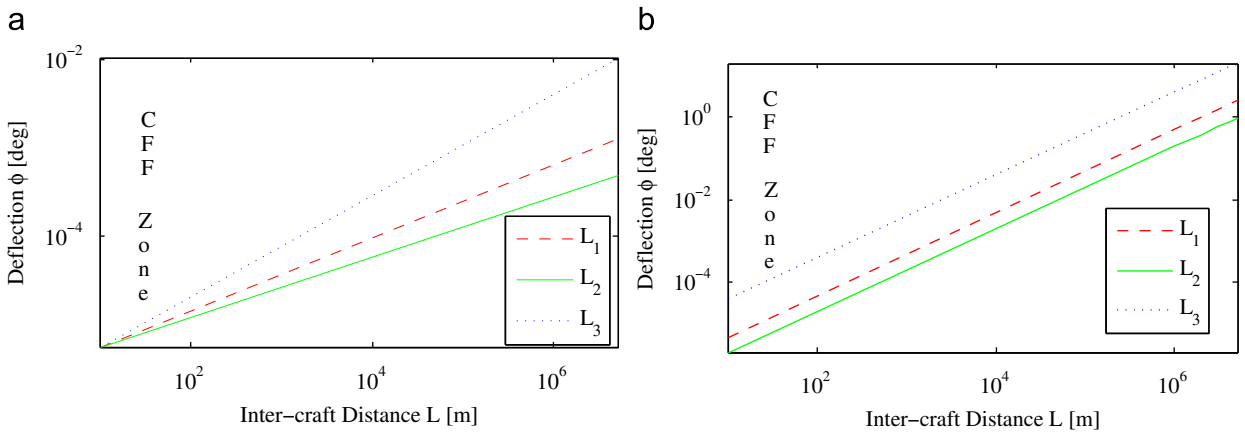

Fig. 11. Deflection for an asymmetric mass distribution. (a) $\chi = 0.49975$, (b) $\chi = 0.0001$.

The solutions of Eq. (52) give the nongreat-circle equilibria and it can be shown that such nongreat-circle equilibria exist only if $m_1 \neq m_2$. The nongreat-circle equilibria formulation is independent of the tether force between the spacecraft and is thus useful for analyzing the equilibria for a range of spacecraft separation distances with the formation at the libration points. Similar to the solution procedure followed for a two-body system, Eq. (52) is expressed in terms of one variable θ, the angle between $\boldsymbol{R}_c$ and the x-axis of the rotating frame.

At the Earth–Moon collinear libration points, the effect of nongreat-circle equilibria on a two-craft formation is studied as a function of spacecraft separation distance L and mass distribution ratio χ defined in Eq. (31). The spacecraft separation distances range from 10 m to 5000 km with the formation center of mass distances fixed at the libration points L_1–L_3. Fig. 11 shows the numerical solutions for a range of spacecraft separation distances. For spacecraft separated by more than 5000 km at L_1 and L_2, a deflection of about 1 from the vertical to the orbital plane is observed. For such large separation distances, a deflection of about 10 is observed at L_3. This is due to L_3 being close to Earth compared to that of L_1 and L_2. On the other hand, for short separation distances the deflection becomes negligible. For instance, Coulomb formations are feasible at the libration points with the spacecraft separation distances ranging from 10 to 30 m due to the reduced range of the Debye length. As shown in Fig. 11(a), for Coulomb formation distances at L_1–L_3, the deflection from normal is less than 10^{-6} degrees. From Fig. 11(b), mass asymmetry of the two craft also yielded negligible effect on the attitude deflection at such short separation distances. Consequently, at libration points, although the orbit-attitude coupling effects dominate for large spacecraft separation distances on the order of thousands of kilometers such effects can be ignored for short separation distances such as in Coulomb formations.

6. Conclusions

In this paper, the relative equilibria of a two-craft formation moving in a two-body system and a three-body system are discussed. A general framework of two-craft connected by an elastic tether force is studied with an emphasis on a virtual Coulomb tether as a special case. The orbit-attitude coupling effects should be considered for large spacecraft separation distances; for LEO, greater than tens of kilometers, for GEO, hundreds of kilometers, and at libration points, tens of thousands of kilometers. Such coupling effects can be ignored for shorter spacecraft separation distances. For example, previous Coulomb formation flying work used the simple principle axes condition. The negligible nongreat-circle effects shown in this paper for smaller inter-craft separation distances validates this assumption for Coulomb tether applications. Consequently, for a charged two-craft formation, the principal axis condition is very good for genetic algorithms which seek approximate equilibrium answers. However, for full nonlinear solutions, these effects can be taken into consideration. Moreover, this paper presents the relative equilibria of a two-craft formation at all five libration points and also numerically shows that nongreat-circle effects exist at the Earth–Moon collinear libration points. Interestingly, in the restricted three-body system, a tether force is required for the along-track equilibrium, however, no tether force is necessary in the restricted two-body system. Furthermore, the results obtained in here could be used to investigate the linearized dynamics and stability of a 2-craft Coulomb tether formation at libration points.

Appendix A. Lie Groups

To explain the terminology used in this paper, basic properties and definitions of Lie Groups are introduced here. Refs. [18,19] present these concepts in detail.

Definition 1 (*Group of transformations*). A group of transformations G is an aggregate set of transformations g_i such that the following properties are satisfied:

(i) It contains the identity transformation.
(ii) Corresponding to each transformation g_l there is an inverse transformation g_l^{-1}.
(iii) The composition of transformations holds $g_l g_k \in G$ and the associativity rule $(g_i g_j)g_k = g_i(g_j g_k)$ is satisfied.

For instance, the set of nonsingular linear transformation matrices forms a group as all the above three properties are satisfied. Another important example is the symmetry group of a rigid body. To maintain the symmetry of a rigid body, symmetry groups or symmetry transformations gives rise to the set of all distance preserving transformations which transforms the position of the body but preserves the distance between all pairs of points of the rigid body.

Definition 2 (*Lie group*). A Lie group is a smooth manifold G that has a group structure consistent with its manifold structure such that the group operation and its inversion are smooth maps between manifolds. A matrix representing a rotation about an axis through an angle is an example of a Lie group. The three-dimensional rotation group $\boldsymbol{SO}(3)$ is defined as

$$\boldsymbol{SO}(3)=\{\boldsymbol{C}:\mathbf{R^3}\rightarrow\mathbf{R^3}\text{ linear, }\boldsymbol{C}^T\boldsymbol{C}=E\text{ and }\det\boldsymbol{C}=1\}$$

Lie groups describe continuous symmetries in physical systems using its Lie algebra $\boldsymbol{g}^*$ for its calculations. A Lie algebra is a vector space and uses linear algebra to study Lie groups. For example, $\boldsymbol{SO}(3)$ is a Lie group and is characterized by its Lie algebra. A Lie group G and its Lie algebra $\boldsymbol{g}^*$ are related in a manner similar to which a flow and the associated vector field are related. The corresponding vector field $\boldsymbol{v}$ on a flow $\boldsymbol{\Phi}(\boldsymbol{x},t)$ given by

$$\boldsymbol{v}(\boldsymbol{x})=\left.\frac{\mathrm{d}}{\mathrm{d}t}\right|_{t=0}\boldsymbol{\Phi}(\boldsymbol{x},t),$$

is called the infinitesimal generator of the flow.

Let $\boldsymbol{so}(3)$ be the set of skew-symmetric matrices defined by

$$\boldsymbol{so}(3)=\{\hat{\xi}:\mathbf{R^3}\rightarrow\mathbf{R^3},\text{ linear }|\hat{\boldsymbol{\xi}}+\hat{\boldsymbol{\xi}}^T|=0\}$$

where $\boldsymbol{\xi}=(\xi_1,\xi_2,\xi_3)$ is a vector and $\hat{\boldsymbol{\xi}}$ is

$$[\hat{\boldsymbol{\xi}}]=\begin{bmatrix}0 & -\xi_3 & \xi_2\\ \xi_3 & 0 & -\xi_1\\ -\xi_2 & \xi_1 & 0\end{bmatrix}$$

This set $\boldsymbol{so}(3)$ forms the Lie algebra of $\boldsymbol{SO}(3)$ given as $\hat{\boldsymbol{\xi}}\boldsymbol{r}=\boldsymbol{\xi}\boldsymbol{r}$ for any $\boldsymbol{r}\in\mathbf{R^3}$. If we define the Lie algebra isomorphism between the space $\mathbf{R^3}$ and $\boldsymbol{so}(3)$ by $\boldsymbol{\xi}\mapsto\boldsymbol{so}(3)$ then the matrix exponential $e^{\hat{\xi}t}$ is a rotation about $\boldsymbol{\xi}$ by the angle $\|\boldsymbol{\xi}\|t$ in the form

$$\boldsymbol{C}(t)=e^{\hat{\boldsymbol{\xi}}t}.$$

References

[1] L.B. King, G.G. Parker, S. Deshmukh, J.-H. Chong, Spacecraft formation-flying using inter-vehicle coulomb forces, Technical Report, NASA/NIAC, January 2002, http://www.niac.usra.edu.

[2] L.B. King, G.G. Parker, S. Deshmukh, J.-H. Chong, Study of interspacecraft Coulomb forces and implications for formation flying, AIAA Journal of Propulsion and Power 19 (3) (2003) 497–505.

[3] A.K. Misra, J. Bellerose, V.J. Modi, Dynamics of a tethered system near the Earth–Moon Lagrangian points, in: Proceedings of the 2001 AAS/AIAA Astrodynamics Specialist Conference of Advances in the Astronautical Sciences, vol. 109, Quebec City, Canada, 2002, pp. 415–435.

[4] B. Wong, R. Patil, A. Misra, Attitude dynamics of a rigid body around the Lagrangian points, AIAA 2006-6653, 2006.

[5] L.S. Wang, J.H. Maddocks, P.S. Krishnaprasad, Steady rigid-body motions in a central gravitational field, Journal of the Astronautical Sciences 40 (4) (1992) 449–478.

[6] J.A. Beck, Relative equilibria of a rigid satellite in a central gravitational field, Ph.D. Thesis, Air Force Institute of Technology, Wright-Patterson AFB, OH, September 1997, aFIT/DS/ENY/97-6.

[7] H. Schaub, J.L. Junkins, Analytical Mechanics of Space Systems, AIAA Education Series, Reston, VA, 2003.

[8] S.F. Cheng, L.S. Li-Sheng Wang, Relative equilibria and stabilities of spring-connected bodies in a central gravitational field, Celestial Mechanics and Dynamical Astronomy 63 (3–4) (1995) 289–312.

[9] H. Schaub, G.G. Parker, L.B. King, Challenges and prospect of Coulomb formations, in: AAS John L. Junkins Astrodynamics Symposium, College Station, TX, 23–24 May 2003, Paper No. AAS-03-278.

[10] G.G. Parker, C.E. Passerello, H. Schaub, Static formation control using interspacecraft Coulomb forces, in: Second International Symposium on Formation Flying Missions and Technologies, Washington, DC, 14–16 September 2004.

[11] E.G. Mullen, M.S. Gussenhoven, D.A. Hardy, SCATHA survey of high-voltage spacecraft charging in sunlight, Journal of the Geophysical Sciences 91 (1986) 1074–1090.

[12] C.C. Romanelli, A. Natarajan, H. Schaub, G.G. Parker, L.B. King, Coulomb spacecraft voltage study due to differential orbital perturbations, AAS/AIAA Space Flight Mechanics Meeting, Tampa Florida, 22–26 January 2006, Paper No. AAS 06-123.

[13] H. Schaub, C.D. Hall, J. Berryman, Necessary conditions for circularly-restricted static Coulomb formations, AAS Journal of Astronautical Sciences 54 (3–4) (2006) 525–541.

[14] J. Berryman, H. Schaub, Static equilibrium configurations in GEO Coulomb spacecraft formations, AAS/AIAA Space Flight Mechanics Meeting, Copper Mountain, CO, 23–27 January 2005, Paper No. 05-104.

[15] J. Berryman, H. Schaub, Analytical charge analysis for 2- and 3-craft Coulomb formations, AIAA Journal of Guidance, Control and Dynamics 30 (6) (2007) 1701–1710.

[16] H. Vasavada, H. Schaub, Analytic solutions for equal mass 4-craft static Coulomb formation, Journal of Astronautical Sciences 56 (1) (2008) 7–40.

[17] L. Pettazzi, H. Krüger, S. Theil, D. Izzo, Electrostatic forces for satellite swarm navigation and reconfiguration, Technical Report, ESA, Doc.No.: ARI-SS-FP-ZAR-001, 2006.

[18] H. Goldstein, Classical Mechanics, second ed., Addison-Wesley, Reading, 1980.

[19] J.E. Marsden, T.S. Ratiu, An Introduction to Mechanics and Symmetry, A Basic Exposition of Classical Mechanical Systems, Springer-Verlag, New York, Heidelberg, Berlin, 1994.